JEE Journal of Ecological Engineering

Journal of Ecological Engineering, 2025, 26(3), 63–76
https://doi.org/10.12911/22998993/199464
ISSN 2299–8993, License CC-BY 4.0

Received: 2024.12.06
Accepted: 2025.01.13
Published: 2025.02.01

Process production sorbitol with photonanocatalysis manganese ferrite based

Rina Krisnayana[1*], Gunawan Nugroho[1], Totok Ruki Biyanto[1]

[1] Department of Engineering Physics, Sepuluh Nopember Institute of Technology, Surabaya, Indonesia
* Corresponding author's e-mail: rina_krisnayana@yahoo.co.id

ABSTRACT

The largest biomass in Indonesia is rice straw, where the largest content is cellulose. Cellulose can convert to sorbitol. This sorbitol useful for various industries, such as the industry chemical, textile, cleaning, control dust, packaging, agriculture and materials burnt. In this study, we produced sorbitol from rice straw by using multistage is hydrolysis NaOH continued photonanocatalyst manganese ferrite based ($MnZnFe_2O_4$, $MnCuFe_2O_4$ and $MnLaFeO_3$). The aim is to obtain sorbitol from rice straw with novelty use photonanocatalyst manganese ferrite based ($MnZnFe_2O_4$, $MnCuFe_2O_4$ and $MnLaFeO_3$). This study provides results that photonanocatalyst of $MnZnFe_2O_4$, $MnCuFe_2O_4$ and $MnLaFeO_3$ can used to convert cellulose into sorbitol. Based on the results of scanning electron microscopy (SEM), Fourier transform infrared spectroscopy (FTIR), X-Ray diffraction (XRD) and thermo gravimetric analysis (TGA), it shows by using multistage is hydrolysis NaOH continued photonanocatalyst of $MnZnFe_2O_4$, $MnCuFe_2O_4$ and $MnLaFeO_3$, sorbitol successfully obtained from rice straw. Conversion cellulose and selectivity optimum on use $MnLaFeO_3$ 125 W with an exposure time of 60 minutes, where the results were influenced by the promoter metal, UV light power and exposure time. More UV light power and longer exposure time give higher conversion cellulose and selectivity sorbitol. Order reaction photonanocatalyst reaction conversion cellulose to sorbitol using nano catalyst $MnLaFeO_3$ is 0.4, the value constant reaction photocatalysis (kr) is 1.3014 $Lg^{-1}.min^{-1}$ and the value Langmuir-Hinshelwood constant (K) is 0.0092 Lg^{-1}. Characterization product sorbitol, the morphology of sorbitol through SEM scan shows that sorbitol is granular. FTIR shows that sorbitol has the following characteristics: group function alcohol (-OH) and alkyl (-CH). XRD reveals that the sorbitol produced is amorphous sorbitol. TGA shows that % heavy experience degradation along with the rise temperature, where sorbitol begins to undergo degradation at a temperature of 200 °C and a maximum at a temperature of 357 °C.

Keywords: rice straw, sorbitol, photonanocatalyst, multistage, manganese ferrite.

INTRODUCTION

Indonesia is the largest 5th producer biomass in the world. In Indonesia, the potential biomass the biggest is rice straw (Energy Outlook, 2021). Rice straw in its use, no influence chain food, because rice straw no can eaten (Londoño-Pulgarin et al., 2021). Main content straw rice is cellulose (Ramos et al., 2023). Rice straw contain cellulose (40–50%), hemicellulose (20–30%) and lignin (10–18%) (Guo et al. 2020), cellulose trapped in the matrix hemicellulose-lignin, which makes its separation very difficult (Rocha et al., 2020; Guo et al., 2020). Cellulose can converted into sorbitol (Zhang et al., 2023). This sorbitol useful for various industry. In chemical industry, sorbitol is used as a solvent in various application (Dias et al., 2022). In the textiles industry, sorbitol can used in manufacturing textile as an agent binder or lubricant in the coloring or dyeing process (Sravan and Spandana, 2021). In cleaners industry, sorbitol is used in cleaners house ladder (Deshmukh et al., 2014). In controller dust industry, sorbitol is used as a thickening agent binder dust. With its properties that can get moisture, sorbitol helps withhold dust to stay down and not flying into the air (Kusnierek et al., 2024). In packaging industry, sorbitol is used to coat material packaging or as an ingredient additional in packaging product sensitive to humidity, because

his ability to maintain moisture and protect product from drought (Paudel et al., 2023). In the field of agriculture, sorbitol is used in the formulation fertilizer or pesticide to help stabilize mixture material active and easy implementation product to plant (Production, 2008). Sorbitol also use as raw material in biofuel production (Torres-Mayanga et al., 2019).

Conversion cellulose to sugar alcohol can carried out by UV *light* photocatalysis using TiO_2 catalyst (Yu et al., 2017), $NiCuFe_2O_4$ catalyst (Rumondang, 2017), $NiZnFe_2O_4$ catalyst (Safitri, 2018), $LaCrO_3$ catalyst (Situmeang et al., 2019), $Ni/LaFeO_3$ catalyst (Iervolino et al. 2021) and catalysts ZnO (Cumba et al., 2022). Photocatalysis has the advantage that is friendly environment (Kumari et al., 2023), can be recycled repeat (Kumari et al., 2023), stable, easy separated (Tahir et al., 2020) and many again superiority other. Mn can used as a photocatalyst in several reaction photocatalytic, photonanocatalysis Mn-based has advantage compared to catalyst based on expensive metals such as titanium or platinum, because lower costs and high stability. Manganese is more affordable and abundant in a way experience compared to platinum or gold, making it more economical. Some compound Mn good stability under conditions reaction photocatalytic.

Due to this reason that, this research conducted production of sorbitol from rice straw with a multistage process, is hydrolysis NaOH continued photonanocatalyst based on manganese ferrite. The novelty is use photonanocatalyst of $MnZnFe_2O_4$, $MnCuFe_2O_4$ and $MnLaFeO_3$ to convert cellulose into sorbitol. Based on the evaluation results, the next will chose catalyst that produces optimum conversion cellulose and selectivity sorbitol. Furthermore, kinetics conversion cellulose use catalyst manganese ferrite with the best modification will studied with variables reaction like concentration cellulose and exposure time. Besides that, identification product also to be considered.

METHODOLOGY

Material

In this study, biomass is rice straw. This rice straw came from Rambutan District, Banyuasin Regency. South Sumatra Indonesia. NaOH is NaOH ≥ 99.0% (E-Merck). H_2SO_4 used for testing cellulose content is H_2SO_4 98% (E-Merck). $NaClO_2$ is used for stage bleaching is $NaClO_2$ 80% Sigma-Aldrich. Materials nano catalyst is $Mn(NO_3)_2.4H_2O$ 98% (E-Merck), $Cu(NO_3)_2 \cdot 3H_2O$ 99% (E-Merck), $Fe(NO_3)_3.9H_2O$ 98% (Pallav), citric acid 99% (Sigma-Aldrich), $Zn(NO_3)_2 \cdot 6H_2O$ 99% (E-Merck) and $La(NO_3)_3 \cdot 6H_2O$ 99% (Sigma-Aldrich).

Preparation cellulose from rice straw

Preparation cellulose from rice straw through 2 stages that is pre-treatment and delignification. At pre-treatment, rice straw destruction with mechanical 5000 rpm, then soaked in water for 6 hours, then mixed with 7 %wt NaOH, then reflux at 80 °C for 5 hours. This is to remove lignin and hemicellulose from rice straw and to purify cellulose. Next stage is delignification. The delignification stage is the results of the stage pre-treatment filtered and residue washed with hot water, then residue dried in the oven, then added 5.25% $NaClO_2$, then reflux at 110 °C for 4 hours. The results left until room temperature, then filtered and residue washed with water until obtained solid white cellulose.

Preparation of nano catalysts

Advantage use nano catalyst is the presence of wide more surface so that area contact larger. Nano catalysts in this study were made using sol gel method. Advantages from sol gel method is to produce catalysts with nano size and higher purity.

Nano catalyst $MnCuFe_2O_4$

Stages making nano catalyst $MnCuFe_2O_4$ is:

1. Mixing $Mn(NO_3)_2 \cdot 4H_2O$ in water, $Cu(NO_3)_2 \cdot 3H_2O$ in water and $Fe(NO_3)_3 \cdot 9H_2O$ in water with a molar ratio of Mn : Cu : Fe = 1 : 1 : 2.
2. Add sour citric into the solution point a mixture with molar ratio of metal ions solution a:sour citrate = 1 : 1 and solution the stirred with a magnetic stirrer until homogeneous.
3. Mixture heated at temperature 80 °C to in gel form.
4. The gel that is formed dried to remove water or solvents others. This process produces xerogel which is a porous material.
5. Xerogel is ground until smooth and next calcined at 600 °C. Temp beginning calcination at 30 °C, then temperature increased by 2 °C / minute to 120 °C, temperature detained for 2 hours, forwarded heating to 350 °C. and then

detained for 2 hours, then temperature raised back to 600 °C, the temperature detained for 2 hours. Then stopped and silenced until temperature room.

Nano catalyst $MnLaFeO_3$

Stages making nano catalyst $MnLaFeO_3$ is:

1. Mixing $Mn(NO_3)_2 \cdot 4H_2O$ in water, $La(NO_3)_3 \cdot 6H_2O$ in water and $Fe(NO_3)_3 \cdot 9H_2O$ in water with a molar ratio of Mn : La : Fe = 1 : 1 : 1.
2. Add sour citric into the solution point a mixture with molar ratio of metal ions solution a: sour citrate = 1:1 and solution the stirred with a magnetic stirrer until homogeneous.
3. Mixture heated at temperature 80 °C to in gel form.
4. The gel that is formed dried to remove water or solvents others. This process produces xerogel which is a porous material.
5. Xerogel is ground until smooth and next calcined at 600 °C. Temp beginning calcination at 30 °C, then temperature increased by 2 °C / minute to 120 °C, temperature detained for 2 hours, forwarded heating to 350 °C. and then detained for 2 hours, then temperature raised back to 600 °C, the temperature detained for 2 hours. Then stopped and silenced until temperature room.

Nano catalyst $MnZnFe_2O_4$

Stages making nano catalyst $MnZnFe_2O_4$ is:

1. Mixing $Mn(NO_3)_2 \cdot 4H_2O$ in water, $Zn(NO_3)_2 \cdot 6H_2O$ in water and $Fe(NO_3)_3 \cdot 9H_2O$ in water with a molar ratio of Mn : Zn : Fe = 1 : 1 : 2.
2. Add sour citric into the solution point a mixture with molar ratio of metal ions solution a: sour citrate = 1:1 and solution the stirred with a magnetic stirrer until homogeneous.
3. Mixture heated at temperature 80 °C to in gel form.
4. The gel that is formed dried to remove water or solvents others. This process produces xerogel which is a porous material.
5. Xerogel is ground until smooth and next calcined at 600 °C, temperature beginning calcination at 30 °C, then temperature increased by 2 °C/minute to 120 °C, temperature detained for 2 hours, forwarded heating to 350 °C and then detained for 2 hours, then temperature raised back to 600 °C, the temperature detained for 2 hours. Then stopped and silenced until temperature room.

Characteristics nano catalyst

Characterization by X-Ray diffraction

Nano catalysts $MnCuFe_2O_4$, $MnLaFeO_3$ and $MnZnFe_2O_4$ results synthesis characterized with use XRD for structure crystals and crystallinity from nano catalyst. Nano catalysts $MnCuFe_2O_4$, $MnLaFeO_3$ and $MnZnFe_2O_4$ results synthesis placed in the sample holder provided. Data collection with XRD instrument is used source Cu Kα radiation (1.54Å) and measurements corner from 2θ at 5–90° with a scan interval of 0.017°.

Measurement specific surface area and pore volume

Measurement specific surface area (SBET), pore volume and analysis distribution pore solid nano catalysts $MnCuFe_2O_4$, $MnLaFeO_3$ and $MnZnFe_2O_4$ by the method adsorption-desorption of N_2 at temperature 77K in a state vacuum. Before measurement wide surface specific and pore volume, a degassing process was carried out with N_2 a temperature of 300 °C for 3 hours to remove gases adsorbed by the sample. The data obtained then processed with the Quantachrome Nova program.

Activity test photonanocatalyst

Conversion cellulose to sorbitol

Activity test photonanocatalyst on nano catalysts did to conversion cellulose into sorbitol. As much as 10 grams cellulose mixed into 100 mL of distilled water, then added nano catalyst as much as 1 gram and hydrogen gas is flowed at a rate of 10 mL/ minute. After that, it is installed UV-light, where position UV-light with a range distance 10–15 cm to the surface reactor. Variable UV-light power used were 60 W and 125 W. Exposure time is 30, 45 and 60 minutes. The product did analysis cellulose content by Datta method and analysis sorbitol content using HPLC instrument.

Cellulose analysis using the Datta method

From the results of point Conversion cellulose to sorbitol carried out filtering with paper filter, then weigh (weight a). After weighing did analysis cellulose content by the Datta method. The following is a method for measuring cellulose content used Datta method proposed by Chesson (Chesson, 1981):

- one g of sample dry (weight b) added 150 mL H_2O or alcohol-benzene and refluxed at 100 °C with a water bath for 1 hour,
- the result filtering, residue washed with 300 mL hot water,
- residue dried in the oven until the weight constant and then weighed (weight c),
- residue added 150 mL H_2SO_4 1 N, then refluxed with a water bath for 1 hour at a temperature of 100 °C,
- the result filtered and washed until neutral (300 ml) and the residue dried until the weight constant. Weight is weighed (weight d),
- residue dry added 100 mL of 72% H_2SO_4 and soaked at room temperature for 4 hours,
- 150 mL of 1 N H_2SO_4 was added and refluxed at 100 °C with a water bath for 1 hour in a cooler,
- residue filtered and washed with H_2O until neutral (400 mL),
- residue heated in an oven at a temperature of 105 °C until the weight constant and weighed (weight e).
- Furthermore, residue ash and weighed (weight f)

Calculation cellulose content use Equation 1 and weight cellulose consumed by Equation 2.

$$Cellulose\ content = \frac{(d-e)}{b} \times 100\% \quad (1)$$

$$Cellulose\ weight\ remainder = \frac{Kadar\ selulos}{100} \times a \quad (2)$$

Analysis of sorbitol by HPLC

From the results of point conversion cellulose to sorbitol carried out analysis to find out sorbitol content with HPLC instrument. The HPLC instrument used has a CLC-NH2 column (4.6 × 250 mm), RID-20A detector, rate the flow is 1 mL/minute at a temperature column 80 °C. Procedure on HPLC using sorbitol standard to determine comparison of retention time with the analyzed sample. 20 µL sorbitol standard 2 g/L was injected into the column. The solution left alone until component solution standard go out from columns and retention time recorded. The mobile phase used was distilled water.

Conversion cellulose and selectivity against sorbitol

Chemical processes, conversion is the ratio how many reactants that have been consumed or size from faction reactants that react. In this study, what is mean reactant is cellulose. The formula calculation conversion cellulose can see in Equation 3.

$$Conversion\ cellulose = \\ = \frac{The\ amount\ of\ cellulose\ consumed}{Amount\ of\ cellulose\ input} \times 100\% \quad (3)$$

Selectivity is a measure efficiency catalyst in converting reactants into the desired products. This selectivity is the fraction from the reacting materials that have been converted into the desired product. In this study, the reactant is cellulose and the desired product is sorbitol. The formula calculation selectivity sorbitol can see in Equation 4.

$$Selectivity\ sorbitol = \\ \frac{Mol\ sorbitol}{Mol\ cellulose\ consumed} \times 100\% \quad (4)$$

Evaluation kinetics use catalyst that has a optimum conversion cellulose

By using same reactor, kinetics reaction process of producing sorbitol using nano catalysts that have optimum conversion cellulose was studied in various concentration cellulose (C_o) is 40 g/L, 60 g/L, 80 g/Land UV *light* exposure time (t) is 5,10, 20, 30, 40, 50 and 60 minutes. At each experiment, did analysis cellulose content, where Equation 2 is heavy remaining cellulose (C).

Determination kinetics to get order reaction, rate reaction photocatalysis and constants reaction photocatalyst. Analysis kinetics reaction photocatalyst is determined by the Langmuir – Hinshelwood kinetic model through plotting the graph (1/ r) vs ($1/C_0$) at different concentrations which can see in Equation 5.

$$\frac{1}{r} = \frac{1}{k_r} + \frac{1}{k_r K}\left(\frac{1}{C_0}\right) \quad (5)$$

where: C_0 is concentration at first cellulose, r is rate reaction photocatalytic and k_r and K is a constant reaction photocatalysis and constants Langmuir-Hinshelwood.

Characterization

After being obtained optimal conversion and selectivity, the resulting sorbitol product did analysis characteristics using SEM, FTIR, XRD and TGA.

Scanning electron microscopy

Scanning electron microscopy (SEM) is used to check structure microscopic and morphological surface sorbitol fibers. SEM was performed at

an acceleration voltage of 20 kV (Fischer et al., 2014). Before scanning coated with gold.

Fourier transform infrared spectroscopy

Fourier transform infrared spectroscopy (FTIR) is used to determine group function (Kunusa et al., 2018). FTIR was performed on a spectrometer running in the range transmission 500–4000 cm^{-1} (Khan et al., 2020). FTIR test was carried out to see existence sorbitol content. FTIR spectrum for the entire test objects are recorded on several the part of the wave band that ranges between 500–4000 cm^{-1} when using ATR method (Lei et al., 2018).

X-Ray diffraction

Analysis X-Ray diffraction (XRD) aim to find out percentage content Crystalline and amorphous in sorbitol. Crystallinity obtained by using diffractometer X-rays equipped with Cu Kα (α = 0.154 nm) in the 2θ range between 5–90, (setting energy battery: 40 kV and 30 mA). Empirical method used to get index crystallinity, Xc sample as shown in Equation 6 (Teixeira et al., 2011)

$$Xc = \frac{I_{002} - I_{am}}{I_{002}} \times 100\% \quad (6)$$

where: I_{002} and I_{am} are the intensities respectively peak material crystal and amorphous. Equation 7 is The Scherrer equation is used to calculate size crystal

$$\tau = \frac{K\lambda}{\beta \cos\theta} \quad (7)$$

where: τ is the dimension upright crystal straight field diffraction with Miller Index hkl, β is the half full width maximum (FWHM) of peak diffraction (Bhattacharya, Germinario, and Winter 2008).

Thermo gravimetric analysis

Thermo gravimetric analysis **(**TGA) measurements of sorbitol samples were carried out on heating rate 10 °C min^{-1} below N_2 atmosphere (20 ml min^{-1}) using TGA. Sample weight 6.0688 mg was taken and stored in a desiccator until weighed. TGA is carried out to observe characteristics degradation sorbitol. The samples were held for 1 min at 40 °C and then heated at a rate of 10 °C min^{-1} from 40 °C to 1000 °C. During the period heating, fraction weight and difference temperature recorded as a function temperature.

RESULTS AND DISCUSSION

Characteristic results of nano catalysts

XRD results

XRD pattern of $MnCuFe_2O_4$ shown in Figure 1(a). The peak reflection according to distance between field characteristics between planes (220), (311), (222), (422), (511) and (440) of spinel ferrite with symmetry cubic $MnCuFe_2O_4$ according to JCPDS 74-2072 data. The pattern is show that material the produced in the form of crystal. The spectrum obtained observe field very reflection intensive and sharp as well as clear. Size average crystallite (D), density dislocation (ρd = $(D)^{-2}$), and strain (ε = β/4tanθ), where β is half maximum full width of XRD peaks of calculated XRD spectrum. By applying the stranded Debye Scherrer equation D = 0.9λ/β cos θ, the size average crystal can was found to be 19.1 nm. The XRD pattern in this study is in accordance with the XRD results of $MnCuFe_2O_4$ in the study Kannapiran et al. (2016) and Khan et al. (2021).

XRD pattern of $MnLaFeO_3$ nano catalyst can be seen in Figure 1 (b). The $MnLaFeO_3$ peak found at 22°, 32°, 40°, 47°, 58° and 68°. This peak accordance with the field diffraction (002), (200), (202), (004), (312) and (400). Size $MnLaFeO_3$ crystals in this study were 20 nm. The XRD pattern in this study was in accordance with the XRD results in the study of Jeong and Raji (Jeong et al., 2018) (Raji et al., 2021).

XRD $MnZnFe_2O_4$ can see in Figure 1 (c). Figure 1(c) shows peaks at 30°, 35°, 43°, 53°, 57°, 62° and 66°. This peak accordance with the field diffraction (220), (311), (400), (422), (511), (440) and (531) (JCPDS card No. 89-7557). These results indicate formation $MnZnFe_2O_4$ spinel nanoparticles with structure cubic. Size crystal nano catalyst $MnZnFe_2O_4$ is 47 nm. The XRD pattern in this study is accordance with the XRD results of $MnZnFe_2O_4$ in the study Kannapiran; Jadhav.

Determination results wide surface and pore volume of nano catalysts

Measurement wide surface from the nano catalysts $MnCuFe_2O_4$, $MnLaFeO_3$ and $MnZnFe_2O_4$ did by the method adsorption nitrogen desorption according to Brunauer-Emmett-Teller (BET) theory. Measurement of pore volume from nano catalysts $MnCuFe_2O_4$, $MnLaFeO_3$ and $MnZnFe_2O$ carried out using the Barreet-Joiner-Halenda

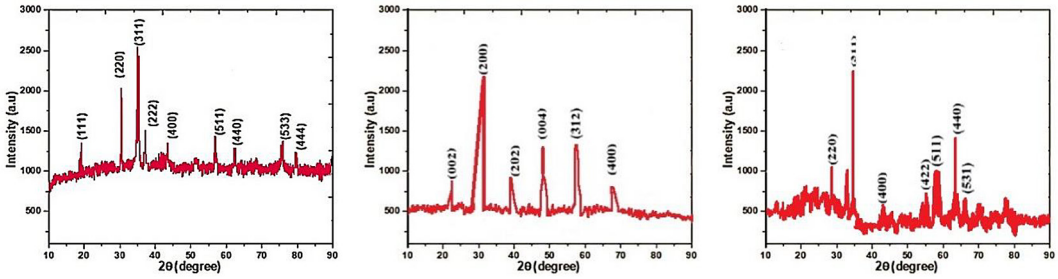

(a) (b) (c)

Figure 1. XRD (a) $MnCuFe_2O_4$, (b) $MnLaFeO_3$, (c) $MnZnFe_2O_4$

(BJH) method. Each nano catalyst has a nitrogen adsorption-desorption yield curve.

The result curve of nitrogen adsorption-desorption of $MnCuFe_2O_4$ show $MnCuFe_2O_4$ follows type IV isothermal curve, where curve isothermal adsorption Type IV is one curve related adsorption with material mesoporous (has pores measuring 2–50 nm). This isothermal marked with existence hysteresis, which indicates mechanism filling different pores compared to with adsorption on the surface non- porous solid. $MnCuFe_2O_4$ is ferrite type, curve isothermal adsorption type IV indicates the material own characteristics mesoporous. This type IV own form the curve that:

- early stage – under pressure relatively low, there is improvement adsorption which represents monolayer adsorption on the surface.
- middle stage – on pressure is happening improvement sharp reflecting filling pore through mechanism capillarity (multilayer adsorption).
- hysteresis – occurs hysteresis loop, indicating filling and emptying different pores. Hysteresis in this type IV generally show existence network structured pores good, which gives characteristic important for $MnCuFe_2O_4$ in application storage energy, catalysts, and adsorption for big molecules.

Isothermal curve adsorption for nano catalysts $MnLaFeO_3$ is Type IV, which has structure mesoporous, indicating characteristics unique related with filling pores.

Here is explanation more details about curve isothermal adsorption for nano catalysts $MnLaFeO_3$:

- initial stage (low pressure): at the stage early under pressure relatively low, adsorption happen in a way gradually. At this stage, molecule absorbed to surface outside and walls in pores mesoporous through monolayer and then multilayer adsorption.
- filling stage (medium pressure): at this stage, occurs improvement more adsorption sharp. This is caused by the condensation process capillaries, where molecules start fill in pores mesoporous materials. This process created significant increase in the number of adsorbed.
- hysteresis loop: characteristics from curve Type IV is existence hysteresis loop that appears on the cycle adsorption and desorption. This loop existence difference mechanism between filling and emptying pore because condensation different capillaries. Hysteresis in $MnLaFeO_3$ show that the material own pores stable mesoporous.
- saturation stage: at higher pressure approach saturation, curve start horizontal, signifying that part big pore has filled. This stage almost no pore empty for filled by adsorbate.

Characteristics hysteresis in curve type IV important for application catalytic and adsorption on $MnLaFeO_3$, because show that the material capable absorb and release molecule with patterns that can predicted.

On the characteristic isothermal adsorption $MnZnFe_2O_4$, this nano catalyst is curve type IV with structure mesoporous. Here is characteristics from curve isothermal adsorption Type IV for $MnZnFe_2O_4$:

- initial stage (relatively low pressure): at the beginning adsorption, molecule adsorbed on the surface outside particles and walls in pores. Monolayer adsorption occurs here and is followed by multilayer adsorption when pressure increase. Increase adsorption at this stage usually stable.
- filling stage (relatively moderate pressure): at higher pressures, molecular start input pores mesoporous through mechanism condensation capillaries, which causes improvement sharp in number adsorbed adsorbate. This

characterizes filling mesoporous material pores.

- hysteresis loop: main features from curve Type IV is hysteresis loop on part adsorption and desorption, which shows that filling and emptying pore happen with different mechanisms. The presence of hysteresis indicates $MnZnFe_2O_4$ has structure stable pores and mesopores that allow the occurrence capillarity.
- saturation stage (relatively high pressure): at very high pressures, curve start horizontal, showing that part big pore has filled. This is to signify that capacity adsorption of material almost reach maximum.

Characteristics hysteresis in curve Type IV for $MnZnFe_2O_4$ very important, especially for application catalyst, because show material ability to absorb and release molecule with a repeating and stable pattern.

Table 1 shows the measurement result wide BET surface area of nano catalysts $MnCuFe_2O_4$, $MnLaFeO_3$ and $MnZnFe_2O_4$. In addition, pore volume measurements are also shown in Table 1. The biggest pore volume is nano catalyst $MnLaFeO_3$. The smallest pore volume is $MnZnFe_2O_4$. Size particles for nano catalysts $MnCuFe_2O_4$, $MnLaFeO_3$ and $MnZnFe_2O_4$ have values < 100 nm, which indicates $MnCuFe_2O_4$, $MnLaFeO_3$ and $MnZnFe_2O_4$ are nano particles.

Influence promoter metal to conversion cellulose and selectivity sorbitol

Figure 2 shows influence type promoter metal to conversion cellulose for produce sorbitol. La promoter resulted the biggest conversion cellulose compared to type other promoter metals. Conversion rate cellulose and selectivity sorbitol each promoter decreased according to order as follows: La > Cu > Zn. La metal gives conversion and selectivity the biggest because La metal can increase acidity Bransted and Lewis on the surface catalyst that helps in the breakdown bond glycosidic in cellulose (Sasidharan et al., 2017). Lanthanum is metals do not have 4f electrons (Cullityc and Graham, 2011). By not having 4f electrons, $MnLaFeO_3$ has the advantage is high reactivity, higher selectivity and more good stability chemistry. Absence of 4f electrons means they have a simple orbital and more available to participate directly in reaction chemistry. This is often produce high activity catalytic (high reactivity). Nano catalysts without 4f electrons, have chemical coordination more controlled, so give higher selectivity in reaction compared to other catalyst. Because the 4f electrons are located deeper and not involved directly in bond chemistry, this element without electrons is more stable in the environment reactions involving oxidation or reduction.

Influence UV light power to conversion cellulose and selectivity sorbitol

Conversion cellulose to sorbitol can carried out using the UV light photocatalysis process (Cumba et al., 2022). Photocatalysis the can done using 60 W UV light, which produces sugar alcohols, is sorbitol, mannitol, xylitol and glucose (Situmeang et al., 2019) (Iervolino et al., 2021). In addition to using 60 W UV light, photocatalysis to convert cellulose into sugar alcohol can also be using 125 W UV light (Yu et al., 2017) (Rumondang, 2017; Safitri, 2018).

Figure 3 shows that bigger UV light power give bigger conversion cellulose and bigger selectivity sorbitol. This is applicable either by using nano catalysts $MnZnFe_2O_4$, $MnCuFe_2O_4$ and $MnLaFeO_3$. Some researcher already to expose that bigger UV light power give bigger conversion (Won et al., 2022; Li et al., 2016; Du et al., 2021). Bigger UV light power give bigger conversion cellulose and bigger selectivity sorbitol, because improvement intensity radiation, reaction photochemistry more efficient, penetration deeper and reaction time faster. With bigger UV light power, intensity the light that hits surface reaction increased. This means more photons available to trigger reaction photochemistry. In reactions involving active photocatalyst against UV,

Table 1. Nano catalyst size

Nano catalyst	Size particle (nm)	Size crystal (nm)	Surface area (m^2/g)	Pore volume (cm^3/g)
$MnCuFe_2O_4$	19	19	30	0.3
$MnLaFeO_3$	20	20	40	0.4
$MnZnFe_2O_4$	47	95	20	0.2

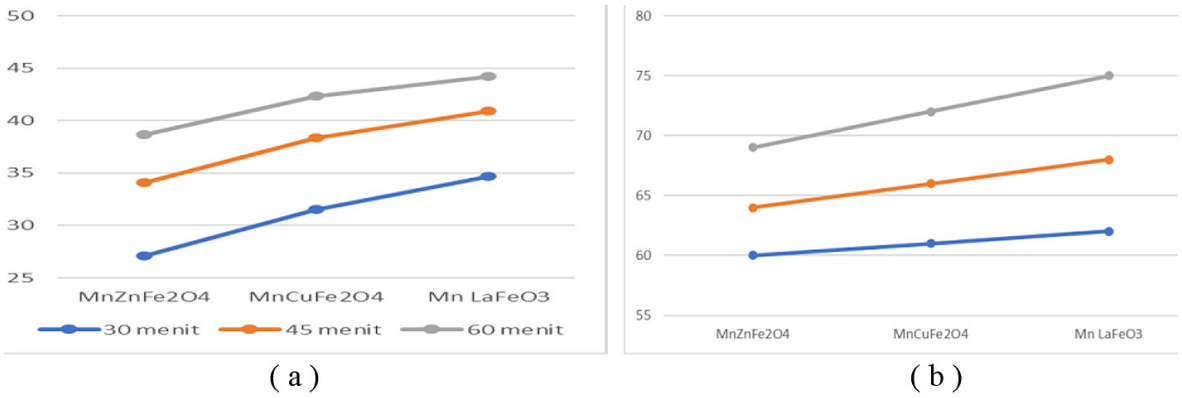

Figure 2. (a) Conversion cellulose photocatalysis 60 W, (b) Selectivity 60 W photocatalysis

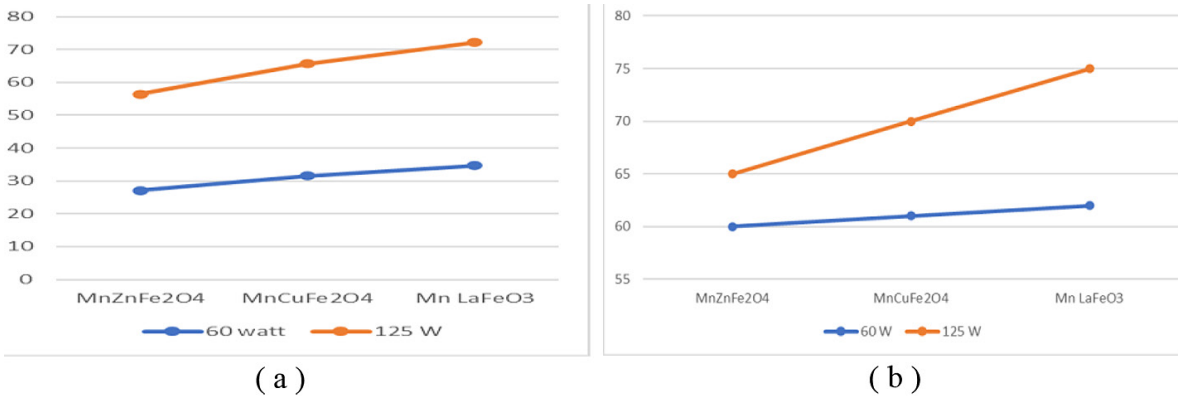

Figure 3. (a) Conversion cellulose photocatalysis for 30 minutes, (b) Selectivity photocatalysis for 30 minutes

photons from UV light will move electrons to the conduction band, creating partner electrons-holes that can participate in the reaction chemistry. More power produced more couple, so that increase rate reaction. UV light with high power can penetrate deeper into the material, resulting in exposed areas radiation increased. This contributed to the increase conversion. With great power, the reaction can faster because improvement energy imparted to a molecule reactant, accelerate termination bonding and formation product new.

Effect of exposure time to conversion cellulose and selectivity sorbitol

Exposure time UV light influence conversion (Simone, 2024; Cuevas-Suárez et al., 2019; Obst et al., 2019; Sianturi et al., 2025). Figure 4 shows longer exposure time UV light give bigger conversion cellulose and bigger selectivity sorbitol. This is applicable for nano catalysts Mn-$ZnFe_2O_4$, $MnCuFe_2O_4$ and $MnLaFeO_3$. Longer exposure time UV light can increase conversion

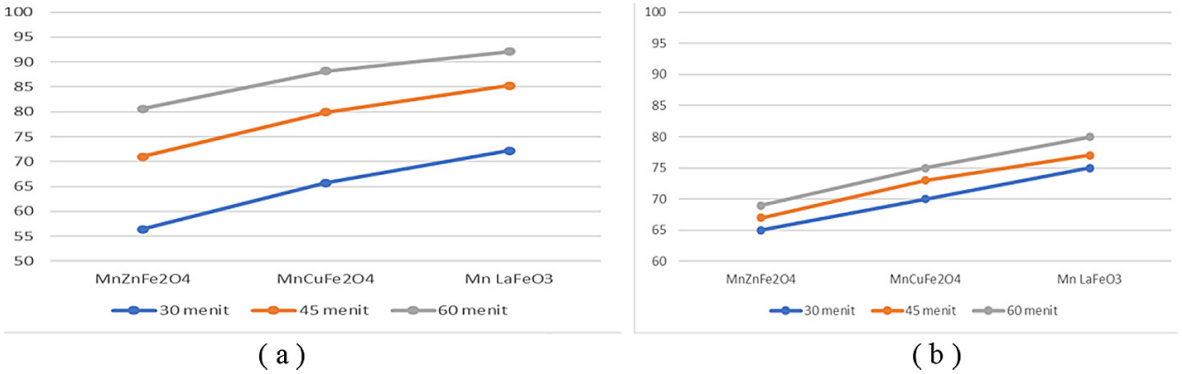

Figure 4. (a) Conversion cellulose photocatalysis 125 W, (b) Selectivity photocatalysis 125 W

cellulose and selectivity sorbitol because this process depends on the activation photonanocatalyst and cleavage bond chemistry certain in cellulose. UV light can activate photonanocatalyst. This activation produces species active free radical or couple electrons-holes, which accelerate reaction decomposition cellulose into glucose. Glucose reduced to sorbitol. Cellulose has a structure complex with bonds glycosidic difficult to broken down. UV light exposure helps weaken or break bond, so that more much sorbitol is produced. With increasing exposure time, the more bond can break down. UV light also encourages reaction chemistry more specific. In the system reaction controlled, longer UV light exposure time give more efficient to direct the way reaction going to the desired product, is sorbitol compared side others product. UV light exposure time provides additional energy to pass obstacle energy activation, so that conversion and selectivity increase.

Kinetic studies photonanocatalysis by nano catalysts that produce conversion optimum cellulose

In this study, optimum conversion cellulose and selectivity sorbitol was obtained by using $MnLaFeO_3$ with a power of 125 W. Calculation rate reaction photocatalysis based on the equation reaction in Equation 8. Reaction rate in a way general can written in accordance Equation 9. By logarithmizing Equation 9, then we get Equation 10.

$$Cellulose \longrightarrow Products \quad (8)$$

$$v = -\frac{dC}{dt} = k \cdot C_{Selulosa}^{m} \quad (9)$$

$$log\ v = m \cdot log\ C_{Cellulose} + log\ k \quad (10)$$

Equation 10 is analyzed by plotting the graph. Where The x-axis is log C and the y-axis is log v. The results of the plot of log v with log $C_{Cellulose}$ got an equation that is equivalent to y = ax + b, with a as the order reaction, x is log $C_{Cellulose}$ which is concentration remaining cellulose, log v as y and log k as b (constant rate reaction). The plot graph between log C and log v is shown in Figure 5(a). The reaction order for various concentration cellulose around 0.4.

To obtain k and K which is constant reaction photocatalysis and constants Langmuir-Hinshelwood, then Equation 5 is carried out analysis. Equation 5 is analyzed by plotting a graph. Where the x-axis is $1/C_0$ and the y-axis is 1/r**.** Co values are 40, 60 and 80 g/L. r value is the inverse value of b in the line equation in Figure 5 (a), where r_{40} = 0.35 g/L min, r_{60} = 0.45 g/L min, and r_{80} = 0.56 g/L min. The resulting graph shown in Figure 5(b). The parameters of the Langmuir-Hinshelwood kinetic model were calculated through intercept and slope obtained from graph in Figure 5 (b), so obtained constant reaction photocatalysis (kr) of 1.3014 $Lg^{-1} \cdot min^{-1}$ and the value Langmuir-Hinshelwood constant (K) is 0.0092 Lg^{-1}.

Identification product photonanocatalysis by nano catalysts that produce optimum conversion cellulose and selectivity sorbitol

SEM results

Sorbitol is obtained from the photonanocatalytic process by nano catalysts which produce optimum conversion cellulose and selectivity sorbitol is $MnLaFeO_3$ under conditions UV light power 125 W and exposure time 60 minutes done SEM analysis. The results of the SEM analysis are shown in Figure 6 (a). From Figure 6 (a) it

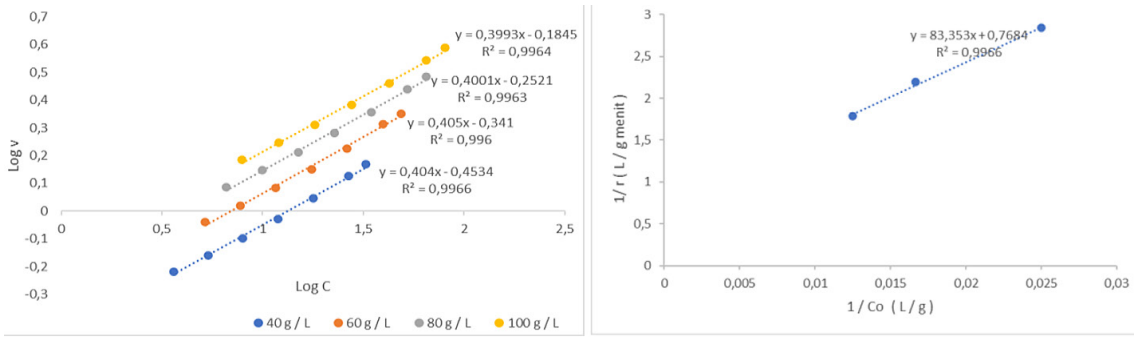

(a) (b)

Figure 5. (a) Order reaction, (b) Constant reaction photocatalysis (kr) and Langmuir-Hinshelwood constant (K)

shows structure microscopic and morphological surface of sorbitol. Sorbitol is granular. This is in accordance with research results Marushka et al. (2022), where are the SEM results of sorbitol in the study Marushka can see in Figure 6 (b).

FTIR results

FT-IR is used to determine group function (Kunusa et al., 2018). Sorbitol obtained from the photonanocatalytic process by nano catalysts which produce optimum conversion cellulose and selectivity sorbitol is $MnLaFeO_3$ under conditions UV light power 125 W and exposure time 60 minutes done FTIR analysis. The results of the FTIR analysis are shown in Figure 7 (a). Figure 7 (a) shows main peak ingredient of sorbitol is peak absorption typical related to the group function alcohol (-OH) and alkyl (-CH). The OH peak is found at around 3200–3600 cm^{-1}, showing vibration upright from OH-CH stretching bonds are at a peak around 2800–3000 cm^{-1} which indicates vibration from CH bonds. The peak at 1400–1450 cm^{-1} is related to CH deformation. The peak at 1000–1200 cm^{-1} indicates vibration from CO bond, which is important for identifying existence alcohol in the sorbitol molecule This is in accordance with research results Basu et al. (2011), where the FTIR results of sorbitol can see in Figure 7 (b).

XRD results

Sorbitol is obtained from the photonanocatalytic process by nano catalysts which produce optimum conversion cellulose and selectivity sorbitol is $MnLaFeO_3$ catalyst under conditions UV light power 125 W and exposure time 60

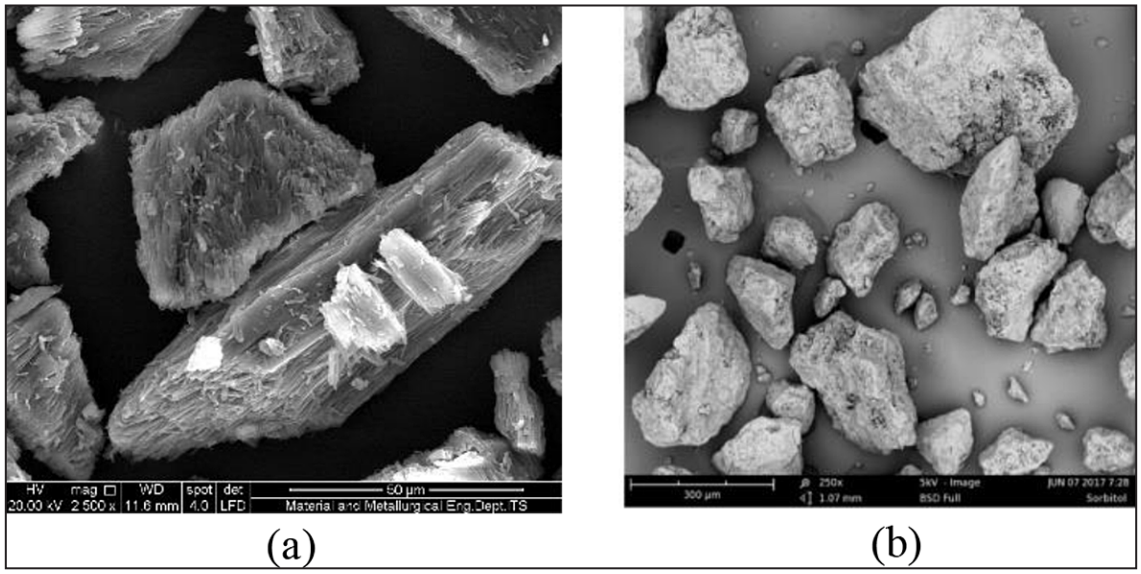

Figure 6. (a) SEM sorbitol experiment at optimum conditions in this research (b) SEM sorbitol research Marushka et al. (2022)

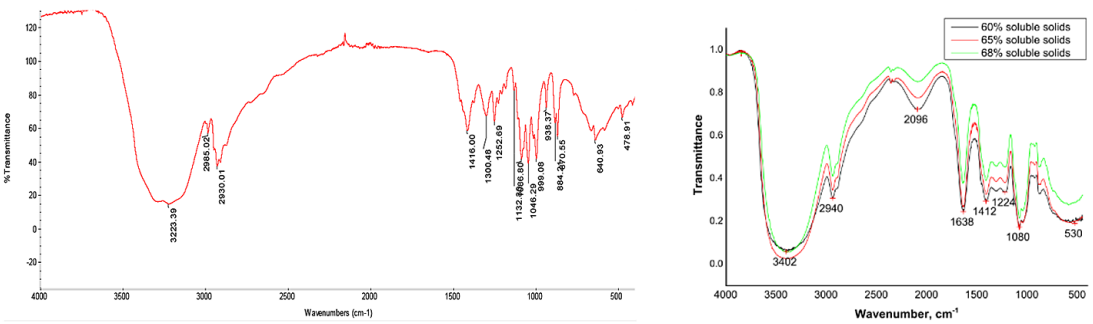

Figure 7. (a) FTIR sorbitol experiment at optimum conditions in this research (b) FTIR sorbitol research Basu et al. (2011)

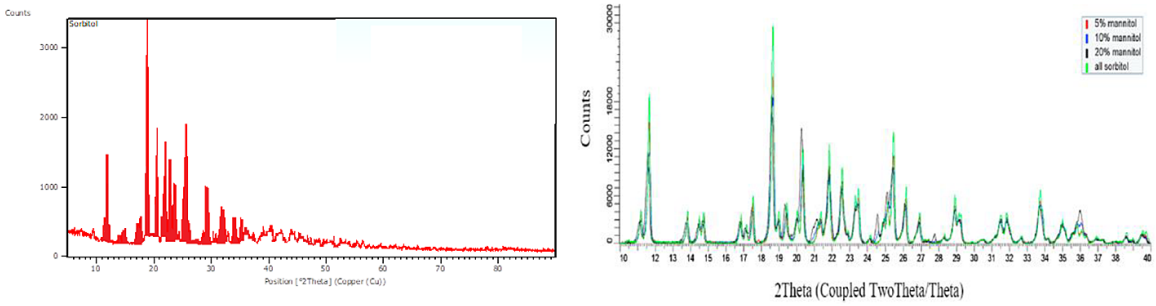

(a) (b)

Figure 8. (a) XRD sorbitol experiment at optimum conditions in this study
(b) XRD sorbitol results by DeJong and Hartel (2021)

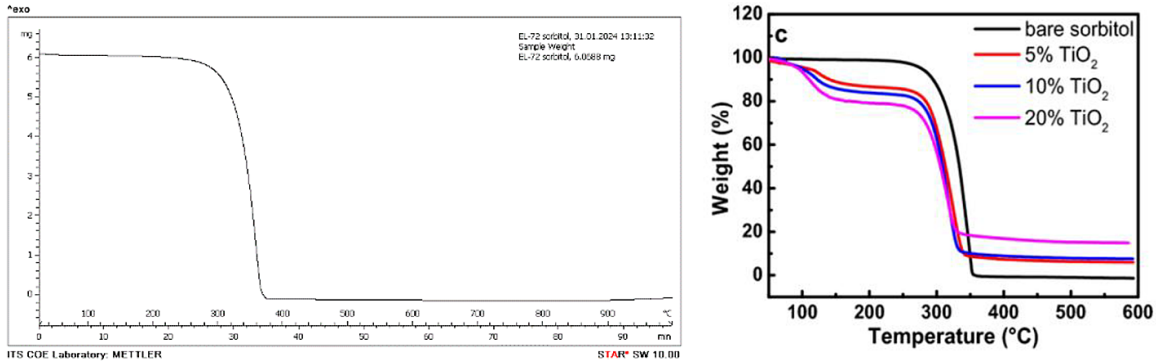

(a) (b)

Figure 9. (a) Experimental sorbitol TGA at optimum conditions in this research
(b) sorbitol TGA results by Saroha et al. (2021)

minutes done XRD analysis. The results of the XRD analysis are shown in Figure 8(a). XRD was used to study behavior crystals and to evaluate connection between structure and characteristics crystals. Sorbitol in structure the molecule shaped amorphous, this means structure sorbitol molecules are random. There is no the regular arrangement of sorbitol molecules, which causes this structure is called amorphous. Sorbitol molecules are distributed in a way random and not to form lattice crystal as in form crystalline. In addition, the ability amorphous sorbitol soluble faster. Amorphous sorbitol easier soluble in water compared to the form crystalline. In addition, Sorbitol is amorphous easier absorb humidity from air. From Figure 8(a), the pattern XRD diffraction of sorbitol shows the peak that corresponds to the peak characteristics sorbitol structure DeJong and Hartel (2021).

TGA results

Sorbitol is obtained from the photonanocatalytic process by nano catalysts which optimum produce conversion cellulose and selectivity sorbitol is $MnLaFeO_3$ under conditions UV light power 125 W and exposure time 60 minutes done TGA analysis. The results of the TGA analysis are shown in Figure 9 (a). The TGA results for sorbitol in this study are in accordance with the TGA results for sorbitol in Jyoti's; Sokker et al. (2005) shown in Figure 9(b). Figure 9 shows that % weight experience degradation (reduction mass) along with the increase temperature. Figure 9 also shows that that sorbitol is starting to experience degradation at a temperature of 200 °C and a maximum at a temperature of 357 °C.

CONCLUSIONS

The conclusions of this study is the photonanocatalysis of $MnZnFe_2O_4$, $MnCuFe_2O_4$ and $MnLaFeO_3$ can used to convert cellulose into sorbitol. Based on the results of SEM, FTIR, XRD and TGA, it shows that by using multistage, is hydrolysis NaOH continued photonanocatalysis of $MnZnFe_2O_4$, $MnCuFe_2O_4$ and $MnLaFeO_3$, sorbitol

was successfully obtained from rice straw. The largest conversion cellulose and selectivity sorbitol obtained use $MnLaFeO_3$ photonanocatalyst 125 W with an exposure time of 60 minutes, where the results were influenced by the promoter metal, UV light power and exposure time. Bigger UV light power and longer exposure time give higher conversion. cellulose and selectivity sorbitol. Order reaction photonanocatalyst reaction conversion cellulose to sorbitol using nano catalyst $MnLaFeO_3$ is 0.4, constant reaction photocatalysis (kr) is 1.3014 $Lg^{-1} \cdot min^{-1}$ and Langmuir-Hinshelwood constant (K) is 0.0092 Lg^{-1}.

REFERENCES

1. Basu, S., Shivhare, U.S., Singh, T.V. and Beniwal, V.S. (2011). Rheological, textural and spectral characteristics of sorbitol substituted mango jam. *Journal of Food Engineering 105*(3): 503–12. http://dx.doi.org/10.1016/j.jfoodeng.2011.03.014
2. Bhattacharya, D., Germinario, L.T and Winter, W.T. (2008). Isolation, preparation and characterization of cellulose microfibers obtained from bagasse. *Carbohydrate Polymers 73*(3): 371–77.
3. Chesson, A. (1981). Effects of sodium hydroxide on cereal straws in relation to the enhanced degradation of structural polysaccharides by rumen microorganisms. *Journal of the Science of Food and Agriculture 32*(8): 745–58.
4. Cuevas-Suárez, C.E., Meereis, C.T.W., D'accorso, N., et al. (2019). Effect of radiant exposure and UV Accelerated Aging on Physico-Chemical and Mechanical Properties of Composite Resins Abstract. 1–9.
5. Cullity, B.D. and Graham, C.D. (2011). Introduction to magnetic materials. *John Wiley & Sons.*
6. Cumba, R.M.T., Ligalig, C.B., Tingson, J.M.D et al. (2022). Photocatalytic activity of cellulose nanocrystals/zinc oxide nanocomposite against thiazine dye under UV and visible light irradiation. *ASEAN Journal of Chemical Engineering 22*(1): 168–77.
7. DeJong, A.E., and Hartel, R.W. (2021). Modulating sorbitol crystallization using impurities. *Journal of Food Engineering 296*(July 2020): 110475. https://doi.org/10.1016/j.jfoodeng.2020.110475
8. Deshmukh, A.G., Gogte, B.B. and Yenkie, M.N. (2014). Liquid laundry detergents based on polymeric surfactants containing sorbitol, starch and sugar syrup. *Der Pharma Chemica 6*(6): 143–48.
9. Dias, M.C.G.C., Farias, F.O., Gaioto, R.C. et al. (2022). Thermophysical characterization of deep eutectic solvents composed by D-Sorbitol, Xylitol or D(+)Xylose as hydrogen bond donors. *Elsevier Journal of Molecular Liquids 354*, 118801, 354.
10. Du, Y., Ziyu, X.A., Li Z., et al. (2021). Visible-to-ultraviolet light conversion: materials and applications. 2000213.
11. Fischer, W.J., Zankel, A, Ganser, C. et al. (2014). Imaging of the formerly bonded area of individual fiber to fiber joints with SEM and AFM. *Cellulose 21*(1): 251–60.
12. Guo, X., Fu, Y., Miao, F. et al. (2020). Efficient separation of functional xylooligosaccharide, cellulose and lignin from poplar via thermal acetic acid/sodium acetate hydrolysis and subsequent kraft pulping. *Industrial Crops and Products 153*(February): 112575. https://doi.org/10.1016/j.indcrop.2020.112575
13. Iervolino, G., Vaiano, V., Sannino, D. et al. (2021). Lafeo3 modified with Ni for hydrogen evolution via photocatalytic glucose reforming in liquid phase. *Catalysts 11*(12): 1–18.
14. Jadhav, S.V., Kim B.M., Lee, H.Y. et al. (2018). Induction heating and in vitro cytotoxicity studies of MnZnFe2O4 nanoparticles for self-controlled magnetic particle hyperthermia. *Journal of Alloys and Compounds 745*(March): 282–91.
15. Jeong, J.H., Song, C.-G., Kim, K.H. et al. (2018). Effect of Mn doping on particulate size and magnetic properties of LaFeO3 nanofiber synthesized by electrospinning. *Journal of Alloys and Compounds 749*: 599–604. https://doi.org/10.1016/j.jallcom.2018.03.352
16. Saroha, J., Mehra, S., Kumar, M. & Sharma, S.N. (2021). Thermo-physical properties of paraffin/TiO_2 and sorbitol/TiO_2 nanocomposites for enhanced phase change materials: A study on the stability issue. *Appl. Phys. A 127*, 127: 916.
17. Kannapiran, N., Muthusamy, A. and Chitra, P. (2016). Effect of $MnCuFe_2O_4$ Content on magnetic and dielectric properties of poly (O-Phenylenediamine)/$MnCuFe_2O_4$ Nanocomposites. *Journal of Magnetism and Magnetic Materials 401*: 345–53.
18. Kannapiran, N., Muthusamy, A. and Meena, S.S. (2021). Study of magnetic and electrical properties of poly(o-Phenylenediamine)/manganese substituted $ZnFe_2O_4$ nanocomposites. *Journal of Inorganic and Organometallic Polymers and Materials 31*(8): 3441–59. https://doi.org/10.1007/s10904-021-02020-2
19. Khan, M.N. et al. (2020). Environmentally benign extraction of cellulose from Dunchi fiber for nanocellulose fabrication. *International Journal of Biological Macromolecules 153*: 72–78. https://doi.org/10.1016/j.ijbiomac.2020.02.333
20. Khan, T.F., Naresh, U., Ramprasad, T. and Kumar, R.J. (2021). Structural, morphological, and

magnetic properties of cobalt-doped nickel ferrite nanoparticles. *Journal of Superconductivity and Novel Magnetism 34*(3): 797–803.

21. Kumari, H. et al. (2023). 234 water, air, and soil pollution a review on photocatalysis used for wastewater treatment: dye degradation. *Springer International Publishing.* https://doi.org/10.1007/s11270-023-06359-9
22. Kunusa, W.R., Isa, I., Laliyo, L.A.R. and Iyabu, H. (2018). FTIR, XRD and SEM Analysis of Microcrystalline Cellulose (MCC) Fibers from Corn Corbs in Alkaline Treatment. *Journal of Physics: Conference Series 1028*(1).
23. Kusnierek, K., Woznicki, T. and Treu, A. (2024). Quality control of wood treated with citric acid and sorbitol using a handheld Raman spectrometer. *Journal of Cleaner Production 434*(November 2023): 139925. https://doi.org/10.1016/j.jclepro.2023.139925
24. Lei, W., Fang, C., Zhou, X. et al. (2018). Cellulose nanocrystals obtained from office waste paper and their potential application in PET packing materials. *Carbohydrate Polymers 181*: 376–85. http://dx.doi.org/10.1016/j.carbpol.2017.10.059
25. Li, L., Sahi, S.K., Penget, M. et al. (2016). Luminescence- and nanoparticle- mediated increase of light absorption by photoreceptor cells: converting UV light to visible light. *Nature Publishing Group* (March). http://dx.doi.org/10.1038/srep20821
26. Londoño-Pulgarin, D., Cardona-Montoya, G., Restrepo, J.C. and Muñoz-Leiva, F. (2021). Fossil or bioenergy? Global fuel market trends. *Renewable and Sustainable Energy Reviews 143*(October 2019).
27. Marushka, J., Hurychová, H., Šklubalová, Z. and Tebbens, J.D. (2022). Flow equations for free-flowable particle fractions of sorbitol for direct compression: An exploratory multiple regression analysis of particle and orifice size influence. *Pharmaceutics 14*(8).
28. Obst, P., Oehlmann, P., Rietzel D., et al. (2019). Investigation of the influence of exposure time on the dual-curing reaction of RPU70 during the DLS process and the resulting part properties.
29. Energy Outlook, BPPT. (2021). Center for Process Industry and Energy Research (PPIPE) Agency for the Assessment and Application of Technology (BPPT) Indonesia Energy Outlook 2021 Indonesian Energy Technology Perspective: Solar Power for Charging Station Energy Supply.
30. Paudel, S., Regmi, S. and Janaswamy, S. (2023). Effect of glycerol and sorbitol on cellulose-based biodegradable films. *Food Packaging and Shelf Life 37.*
31. Production, Crop. (2008). *Sorbitol Octanoate*. 035400: 1–7.
32. Raji, R.K., Ramachandran, T., Muralidharan, M. et al. (2021). Twitching the inherent properties: The impact of transition metal Mn-doped on $LaFeO_3$-based perovskite materials. *Journal of Materials Science: Materials in Electronics 32*(20): 25528–44.
33. Ramos, M., Laveriano, E., Sebasti´an, L.S. et al. (2023). Rice straw as a valuable source of cellulose and polyphenols: Applications in the food industry. *Trends in Food Science and Technology 131*(November 2022): 14–27.
34. Rocha, G.J.M., Andrade, L.P., Martín, C. et al. (2020). Simultaneous obtaining of oxidized lignin and cellulosic pulp from steam-exploded sugarcane bagasse. *Industrial Crops and Products 147*(February): 112227. https://doi.org/10.1016/j.indcrop.2020.112227
35. Rumondang, D. (2017). *Conversion of Nanocellulose into Sugar Alcohol Using Uv-Irradiated Ni-0.9cu0.1fe2o4 Nanocomposites.* Nusantara PGRI University Kediri 1: 1–7. http://www.albayan.ae.
36. Safitri, M. (2018). *Conversion of Corn Cob Waste Cellulose into Sugar Alcohol Using Nanocatalist Ni*. 4: 1–97.
37. Sasidharan, S. (2017). Sol-Gel Lanthanum Phosphate: A Versatile Ceramic Material for Diverse Functional Applications. (June): 285–312.
38. Sianturi, L., Humaidi, S., Sembiring, T. et al. (2024). UV exposure time optimization for enhanced conversion, hardness, and flexural strength in UDMA / TEG-DMA composite resins. *Trends in Sciences 21*(12): 8603.
39. Šimunovi, L., Marić, A.J., Bačić, I. et al. (2024). Applied sciences impact of UV light exposure during printing on thermomechanical properties of 3D-printed polyurethane-based orthodontic aligners.
40. Situmeang, R., Tamba, M., Simarmataet, E. et al. (2019). $LaCrO_3$ nano photocatalyst: the effect of calcination temperature on its cellulose conversion activity under UV-Ray irradiation. *Advances in Natural Sciences: Nanoscience and Nanotechnology 10*(1).
41. Sokker, H.H., Halim A.E.S., Aly, A.S. and Hashem, A. (2005). Grafting DMAEMA into fabrics in cellulosic fiber to remove direct dyes cellulosic fabric wastes grafted with DMAEMA for the removal of direct dyes. (February). *Adsorption Science & Technology.* https://doi.org/10.1260/0263617043026497
42. Sravan, T., and Spandana City. (2021). Sorbitol its applications in different fields. *Agriculture & Food: E-Newsletter 3*(3): 2–4.
43. Tahir, M.B. Iqbal, T., Rafique, M. et al. (2020). Nanotechnology and photocatalysis for environmental applications nanomaterials for photocatalysis. *Elsevier Inc.* https://doi.org/10.1016/B978-0-12-821192-2.00005-X
44. Teixeira, E. de M. et al. (2011). Sugarcane bagasse whiskers: Extraction and characterizations.

Industrial Crops and Products 33(1): 63–66. http://dx.doi.org/10.1016/j.indcrop.2010.08.009

45. Torres-Mayanga, P.C., Lachos-Perez, D., Mudhoo, A. et al. (2019). Production of biofuel precursors and value-added chemicals from hydrolysates resulting from hydrothermal processing of biomass: A review. *Biomass and Bioenergy 130*(September): 105397. https://doi.org/10.1016/j.biombioe.2019.105397
46. Won, J., Hyun, R. and Boo, J.-H. (2022). Enhancement of UV-light harvesting in perovskite solar cells by internal down-conversion with Eu-Complex hole transport layer. *Energy Reports 8*: 214–22. https://doi.org/10.1016/j.egyr.2022.08.125
47. Yu, Y. et al. (2017). UV and visible light photocatalytic activity of Au/TiO_2 nanoforests with anatase/rutile phase junctions and controlled au locations. *Scientific Reports 7*(December 2016): 1–13. http://dx.doi.org/10.1038/srep41253
48. Zhang, Y., Zhang, G. and Chen, T. (2023). Efficient one-pot conversion of cellulose to sorbitol over ni-based carbon catalysts with embedment structure. *Elsevier Fuel 339*, 1 May 2023, 127447 339.